

Transition nucleon resonance electrocouplings from CLAS data on $\pi^+\pi^-p$ electroproduction off protons

Victor I. Mokeev

*Thomas Jefferson National Accelerator Facility, Newport News, Virginia 23606, USA
Skobeltsyn Nuclear Physics Institute at Moscow State University, Moscow, Leninskie gory 119889, Russia*

Abstract. Electrocouplings of excited proton states with masses less than 1.8 GeV were determined for the first time from the CLAS data on $\pi^+\pi^-p$ electroproduction at photon virtualities $Q^2 < 1.5 \text{ GeV}^2$. Electrocouplings were obtained from a combined fit of all available observables within the framework of a phenomenological reaction model.

Keywords: meson electroproduction, nucleon resonance structure, transition form factors

PACS: PAC number(s): 11.55.Fv, 13.40.Gp, 13.60.Le, 14.20.Gk

INTRODUCTION

Studies of nucleon resonance electrocouplings $\gamma_{virt}NN^*$ from $ep \rightarrow e'\pi^+\pi^-p$ channel represent an important part of the N^* Program with the CLAS detector [1]. The $N\pi$ and $\pi^+\pi^-p$ exclusive electroproduction channels are major contributors in the resonance excitation region with entirely different non-resonant mechanisms. Therefore, they provide independent information on $\gamma_{virt}NN^*$ electrocouplings, that is vital for the reliable extraction of these fundamental quantities. Comprehensive information on $\gamma_{virt}NN^*$ electrocouplings of various excited proton states in a wide range of photon virtualities Q^2 gives access to active degrees of freedom in the N^* structure at various distances. This allow us to explore non-perturbative strong interaction mechanisms, that are responsible for baryon formation. Preliminary results on the Q^2 -evolution of $\gamma_{virt}NN^*$ electrocouplings for excited proton states with masses less than 1.8 GeV are reported. They were obtained for the first time from $\pi^+\pi^-p$ electroproduction off protons [2, 3].

ANALYSIS APPROACH

The CLAS data on $\pi^+\pi^-p$ electroproduction [2, 3] for the first time provided information on nine independent one-fold differential and fully integrated cross sections in each bin of W and Q^2 in a mass range $1.31 < W < 2.1 \text{ GeV}$ and at photon virtualities from 0.25 to 1.5 GeV^2 . Analysis of these data allowed us to establish all essential mechanisms contributing to $\pi^+\pi^-p$ electroproduction in this kinematical area. The presence and strengths of the contributing $\pi^+\pi^-p$ electroproduction mechanisms was established by studying the kinematical dependencies in differential cross sections and their correlations in a variety of available observables. This resulted in the development of meson-baryon reaction model JM for the description of $\pi^+\pi^-p$ electroproduction off protons [4, 5]. The primary objective is to determine $\gamma_{virt}NN^*$ electrocouplings and $\pi\Delta$ and ρp partial hadronic decay widths of N^* 's from a combined fit of all available observables. The model incorporates the full $\pi^+\pi^-p$ production amplitude of the $\pi^-\Delta^{++}$, $\pi^+\Delta^0$, ρp , $\pi^+D_{13}^0(1520)$, $\pi^-P_{33}^{++}(1600)$, $\pi^+F_{15}^0(1685)$ isobar channels and direct double pion production mechanisms, that account for all resonant and non-resonant partial waves combined. Direct double pion production mechanisms describe processes when the final $\pi^+\pi^-p$ state is created without formation of unstable hadrons in intermediate states. Direct 2π production mechanisms, required by general unitarity condition [8], were established for the first time in the analysis of CLAS $\pi^+\pi^-p$ electroproduction data. Implementation of direct 2π production processes into the JM model allowed us to move beyond the isobar approximation for the description of $\pi^+\pi^-p$ electroproduction off protons. The JM model incorporates all N^* 's with masses less than 2.0 GeV that couple to the two pion channel. Resonant amplitudes contribute to $\pi\Delta$ and ρp isobar channels, while the other isobar channels contain only non-resonant mechanisms. Breit-Wigner parametrization for resonance amplitudes, employed in the JM model (the regular Breit-Wigner ansatz), is described in [6, 7]. However, this ansatz does not satisfy unitarity condition in a case, when various N^* states could be mixed in a dressed resonance propagator. Therefore, in the 2010 JM model version the resonant amplitudes were

parametrized using a unitarized Breit-Wigner ansatz, that was initially proposed in [8]. This ansatz was modified to make it consistent with resonant amplitude parametrization adopted in the JM model. The unitarized Breit-Wigner ansatz allowed us to account for transitions between various N^* states in the dressed resonance s-channel propagator and to impose restrictions on resonant amplitudes required by general unitarity condition. Non-resonant amplitudes incorporated into the JM model were presented in the papers [4, 5].

A reasonable description of the $\pi^+\pi^-p$ electroproduction channel was achieved, allowing us to separate resonant and non-resonant contributions to the measured cross sections, which is needed for the evaluation of $\gamma_{virt}NN^*$ electrocouplings.

FITTING PROCEDURE

The N^* electrocouplings and their $\pi\Delta$ and ρp partial hadronic decay widths were obtained from fits to the $\pi^+\pi^-p$ electroproduction data [2, 3] within the framework of JM model [4, 5]. These resonance parameters, as well as parameters describing the non-resonant mechanisms in the JM model were varied simultaneously in the χ^2 minimization. In this way we accounted for correlations of resonant and non-resonant contributions. For each trial set of computed cross sections the $\chi^2/\text{d.p.}$ value was estimated in point by point comparison between measured and computed nine one-fold differential cross sections in all bins of W and Q^2 covered by measurements.

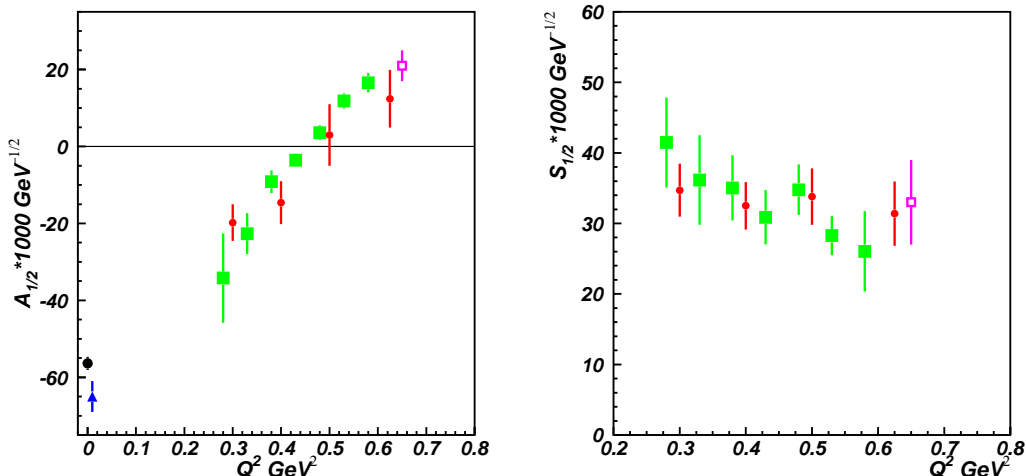


FIGURE 1. $A_{1/2}$ (left) and $S_{1/2}$ (right) electrocouplings of $P_{11}(1440)$ state determined from the CLAS data [3] on $\pi^+\pi^-p$ electroproduction (filled squares) and from $N\pi$ electroproduction [9] (filled circles). Results from a combined analysis of $N\pi$ and $\pi^+\pi^-p$ channels [10] are shown by open squares. Filled circle and triangle at the photon point correspond to CLAS [11] and PDG analyses of $N\pi$ channels, respectively.

$\gamma_{virt}NN^*$ electrocouplings, as well as resonance $\pi\Delta$ and ρp partial hadronic decay widths assigned to selected in the fit calculated cross sections were averaged, giving us the mean values of resonance parameters determined from the data fit. Dispersions in the sets determined in the fit resonance parameters were considered as their uncertainties.

RESULTS

Electrocouplings of the $P_{11}(1440)$ state determined from the analysis are shown in Fig. 1. The error bars include quadratic sums of statistical and systematic uncertainties. We also show electrocouplings of this state obtained from a combined analysis of the data on π^+n and π^0p electroproduction channels [9]. Electrocoupling values extracted from analyses of these exclusive channels are in good agreement. We also found consistent values for electrocouplings of $D_{13}(1520)$ and $F_{15}(1685)$ states determined independently from the two channels. As an example, the $A_{3/2}$ electrocouplings of these states are shown in Fig. 2.

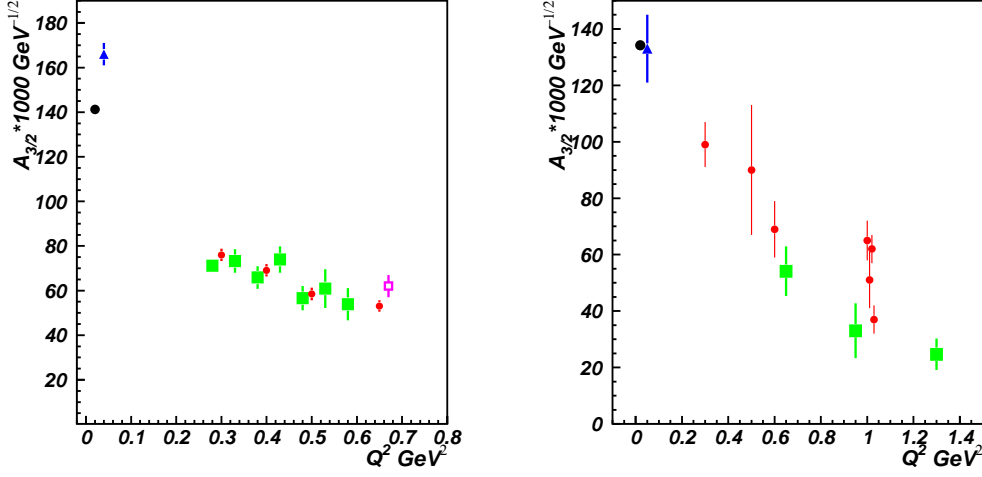


FIGURE 2. The $A_{3/2}$ electrocouplings of $D_{13}(1520)$ (left) and $F_{15}(1685)$ (right) resonances. The results from analysis of $\pi^+\pi^-p$ CLAS data [2, 3] are shown by filled squares. Electrocouplings of $D_{13}(1520)$ state determined from analysis of the CLAS data on $N\pi$ electroproduction [9] and electrocouplings of $F_{15}(1685)$ state obtained from analyses of previously available world data, taken from the compilation [12], are shown by filled circles. Filled circles and triangles at the photon point correspond to CLAS [11] and PDG analyses of $N\pi$ channels, respectively.

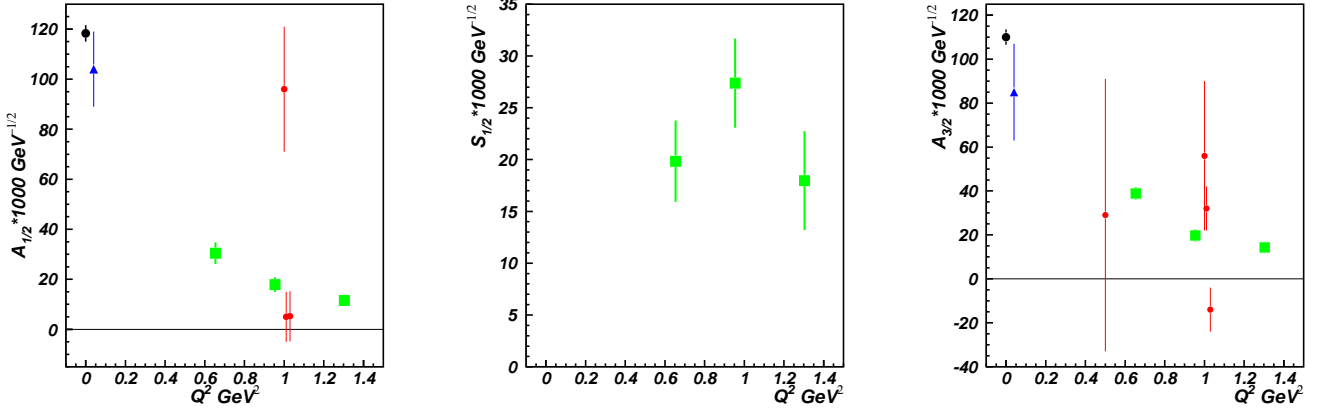


FIGURE 3. Electrocouplings of $D_{33}(1700)$ resonance. Results from analysis of $\pi^+\pi^-p$ CLAS data [2] are shown by filled squares, while filled circles represent the results obtained worldwide from analyses of $N\pi$ electroproduction data, taken from the compilation [12]. Filled circles and triangles at the photon point correspond to CLAS [11] and PDG analyses of $N\pi$ channels, respectively.

$N\pi$ and $\pi^+\pi^-p$ exclusive electroproduction channels represent two major contributors to meson electroproduction in the N^* excitation region with completely different non-resonant mechanisms. The successful description of a large body of observables in these two exclusive channels using nearly the same electrocouplings of $P_{11}(1440)$, $D_{13}(1520)$ and $F_{15}(1685)$ states provides strong evidence for a reliable evaluation of these fundamental quantities.

Many excited states with masses above 1.6 GeV preferably couple to $N\pi\pi$ final states. Therefore, analysis of $\pi^+\pi^-p$ electroproduction is of particular importance to obtain reliable information on high lying N^* states.

Figure 3 shows $D_{33}(1700)$ electrocouplings determined in our analysis in comparison with previously available world data from analyses of $N\pi$ electroproduction. Large uncertainties of previous world data on $D_{33}(1700)$ electrocouplings are related to the fact that $N\pi$ is a minor decay channel (10-20%) of this state, that couples dominantly to

TABLE 1. $\pi\Delta$ and ρp partial hadronic decay widths of $P_{13}(1720)$ state determined from analysis of the CLAS $\pi^+\pi^-p$ electroproduction data [2], employing the regular [6] and the unitarized [8] Breit-Wigner ansatz for resonant amplitudes.

Breit-Wigner ansatz:	$\Gamma_{\pi\Delta}$, MeV	$\Gamma_{\rho p}$, MeV
Regular	1.5 ± 1.1	$114 \pm 12.$
Unitarized	10.9 ± 1.4	83 ± 3.3

$N\pi\pi$ final states (80-90%). Analysis of the $\pi^+\pi^-p$ data [2] within the framework of JM model allowed us to obtain accurate information on electrocouplings of this and also of the $S_{31}(1620)$, $S_{11}(1650)$, $F_{15}(1685)$, and $P_{13}(1720)$ states at photon virtualities from 0.5 to 1.5 GeV². Moreover, longitudinal electrocouplings of these resonances have become available from this analysis for the first time.

In order to examine the effects of resonant amplitude unitarization, we compared resonance parameters determined within the frameworks of the regular [6, 7] and, described above, unitarized Breit-Wigner ansatzs. We found that $\gamma_{virt}NN^*$ electrocouplings determined by employing the regular and the unitarized formulations are consistent with each other. However, unitarization of resonant amplitudes affects substantially $\pi\Delta$ and ρp partial hadronic decay widths of excited proton states. An example is shown in the Table 1, where we compare the $\pi\Delta$ and ρp partial hadronic decay widths of $P_{13}(1720)$ state, obtained from the $\pi^+\pi^-p$ data fit by employing the JM model, that incorporate the regular and unitarized Briet-Wigner ansatzs, respectively.

CONCLUSION AND OUTLOOK

Accurate information on the Q^2 -evolution of $\gamma_{virt}NN^*$ electrocouplings for many excited proton states with masses less than 1.8 GeV and at photon virtualities up to 1.5 GeV² have become available from CLAS data on $\pi^+\pi^-p$ electroproduction. These results open up new opportunities for theory to explore confinement mechanisms in the baryon sector through their manifestation in the structure of excited proton states of various quantum numbers, as it was outlined in [13]. The analysis reported here covers the range of photon virtualities, where both meson-baryon and quark degrees of freedom can be relevant. Our results on high lying N^* electrocouplings for the first time make it possible to explore the transition from meson-baryon to quark degrees of freedom in the structure of excited proton states with masses above 1.6 GeV within the framework of dynamical coupled channel approaches under development in EBAC at Jefferson Lab [14].

REFERENCES

1. V. D. Burkert, AIP Conf. Proc. **1182**, 900 (2009).
2. M. Ripani et al., CLAS Collaboration, Phys. Rev. Lett. **91**, 022002 (2003)
3. G. V. Fedotov et al., CLAS Collaboration, Phys. Rev. C **79**, 015204 (2009).
4. V. I. Mokeev et al., Phys. Rev. C **80**, 045212 (2009)
5. V. I. Mokeev and V. D. Burkert, J. Phys. Conf. Ser. **69**, 012019 (2007).
6. M. Ripani et al., Nucl. Phys. A **672**, 220 (2000).
7. V. I. Mokeev et al., Phys. Atom. Nucl. **64**, 1292 (2001).
8. I. J. R. Aitchison, Nucl. Phys. A **189**, 417 (1972).
9. I. G. Aznauryan et al., CLAS Collaboration, Phys. Rev. C **80**, 055203 (2009).
10. I. G. Aznauryan et al., Phys. Rev. C **72**, 045201 (2005).
11. M. Dugger et al., CLAS Collaboration, Phys. Rev. C **79**, 065206 (2009).
12. V. D. Burkert et al., Phys. Rev. C **67**, 035204 (2003).
13. I. G. Aznauryan et al., JLAB-PHY-09-0993, arXiv:0907.1901 [nucl-th].
14. N. Suzuki, T. Sato, T.-S.H. Lee, JLAB-THY-10-1162, arXiv:1006.2196 [nucl-th].